DOI: http:/dx.doi.org/10.18180/tecciencia.2013.14.3

TECCIENCIA

Braking mechanism for the RCAR protocol in vehicle crash-test trials

Mecanismo de frenado para vehículos de prueba en ensayos de crash test regulados por el protocolo RCAR

Daniel Eduardo Villalobos[1], Carlos Alberto Garzón[2], Jeisson Alexander Gómez[3], Juan Carlos Ovalle[4]

[1]*Escuela Colombiana de Carreras Industriales, Bogotá, Colombia, dvillalobosc@ecci.edu.co*
[2]*Escuela Colombiana de Carreras Industriales, Bogotá, Colombia, cgarzonr@ecci.edu.co*

Received: 14 May 2013 *Accepted: 20 June 2013* *Published: 30 July 2013*

Abstract

This paper shows the design and development of a braking mechanism remotely controlled via pneumatic elements. The objective of the mechanism is to stop test vehicles during ***Crash*** test trials, respecting the protocol governing these test by Global Research Council for automobile repair (RCAR).The research for the construction of such a mechanism covered topics like impact and braking dynamics, automotive crashing test, pneumatics and testing mechanism developed in the center of experimentation and road safety (CESVI) Colombia where it became necessary to build it

Keywords*:** dynamic braking, dynamic impact, ***crash test trials, the braking mechanism, pneumatic.

Resumen

Este trabajo muestra el diseño y desarrollo de un mecanismo de frenado controlado remotamente que funciona mediante elementos neumáticos. Su objetivo es detener vehículos de prueba en los ensayos de *crash test*, respetando el protocolo que regula estos ensayos por el RCAR (Consejo de investigación mundial para la reparación de automóviles). La investigación para la implementación de dicho mecanismo abarcó temas como la dinámica de impacto y de frenado, tipos de pruebas de colisión para automóviles, neumática y pruebas del mecanismo desarrolladas en el centro de experimentación y seguridad vial CESVI Colombia, donde nació la necesidad de construirlo.

Palabras clave: dinámica de frenado, dinámica de impacto, ensayos *crash test*, mecanismo de frenado, neumática

1. Introduction

Representatives of vehicle brands demand the execution of crash-test trials for consumers to evaluate the response of automobiles to collisions [1]. Two types of trials exist: the completely destructive ones in which the vehicle is declared a total loss [2], and those that can be repaired, where the vehicle can be returned to operational conditions; these latter are carried out at low speed. CESVI Colombia is in charge of performing these impact tests at its unique experimental center in Colombia. Low-speed impact tests (Crash Test) [3] were designed to measure and quantify repair costs upon assessing the damage to vehicle when an accident occurs; all this to be certain of the repair characteristics that should be applied in the different vehicle models.

These low-speed impact tests comprise two parts; the first test consists of placing the vehicle on an impact ramp for it to collide against a rigid barrier at 15 km/h ± (1 km/h). The test vehicle is repaired and a second impact test is performed, which consists of placing it on the parked test track, then a moving barrier impacts it at a speed of 15 km/h ± (1 km/h). The objective of the braking mechanism is to stop the inertia of the test vehicles after performing the rear impact test, as

How to cite: Villalobos-Correa, D. *Et al.* ***Braking mechanism for the RCAR protocol in vehicle crash-test trials,*** TECCIENCIA, Vol. 7 No. 14., 23-31**,** 2013 **DOI:** **http:/dx.doi.org/10.18180/tecciencia.2013.14.3**

mentioned in the RCAR protocol version 2.2. [1] [3], besides considering the mechanism as a safety tool that can be of great help to keep the front part of the vehicle from colliding against the frontal barrier. To construct the mechanism, the parameters were analyzed [4]in addition to studying the geometric configuration [4] [5], materials [6], and the control [7] needed to set it into action.

Specialized literature on the topic is focused on solving simulation problems to calculate deformations and speeds of deformation, [8] for example, by studying the amount of energy absorbed and deformation during an impact through image analysis [9] and studies that propose the implementation of passive safety systems onto vehicular driving justifying it through vehicle collision statistics [10]; hence, this specific item of implementing the device is innovative regarding its purpose and which to date has only been implemented at CESVI.

2. Impact tests carried out at cesvi Colombia

The aim of the front and rear low-speed impact tests on the impact ramp is to reproduce as closely as possible collisions in city streets, which occur most frequently while driving. This types of trials are not destructive (RCAR does not consider this type of test as destructive, although some parts of the vehicle are destroyed), which is why the vehicle is repairable for the purpose of performing analyses of repair times and costs. These impact tests are regulated by the RCAR, which stipulates that tests be conducted on production series vehicles not over 3500 kilograms.

2.1 Front impact test

In this impact test, the test vehicle is placed on the impact ramp, where it is pulled by a cable, which is boosted by an electric motor operated from a cockpit; when the test vehicle is launched against the rigid barrier, the condition is that it should be with the ignition in ON position with the gear box free of traction and the emergency brake deactivated. The vehicle should move freely to reach an average speed of 15 Km/h ±1 Km/h.

At the end of the track, the test vehicle collides against the rigid and indestructible barrier that weighs 85 tons and is anchored to eight meters below the track level; the barrier forms a 10° angle with respect to the vehicle's longitudinal axis. The impact takes place on 40% of the vehicle's total front width (Figure 1).

Where:
U = 40% compensation
B = total width of the vehicle
R = 150 mm of radius
F = vehicle test
A = 10° angle

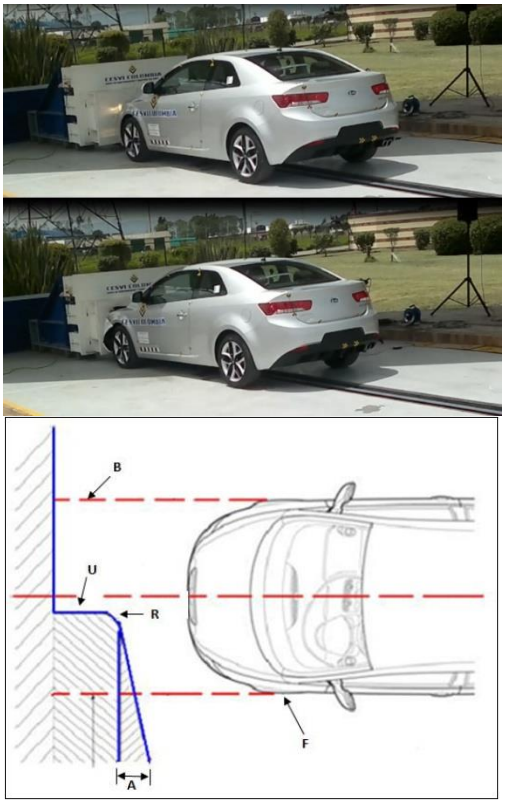

Figure 1. Left: scheme of front impact. Right: images of the front impact test.

2.2 Rear impact test

The rear impact test is carried out with the test vehicle detained and placed on the impact track, at a 10° angle with respect to the track's horizontal; the test vehicle cannot be blocked, meaning that it must be in neutral position and without the parking brake activated.

Thereafter, a moving barrier will impact the rear of the vehicle. The moving barrier is constructed under the standards established by the RCAR, and it is nothing else but a 1400-Kg rolling structure, equipped with a steel frontal plate with normalized dimensions, which is the contact surface that collides with the test vehicle. In this case, the study is conducted by striking 40% of the total rear width of the vehicle toward the right side.

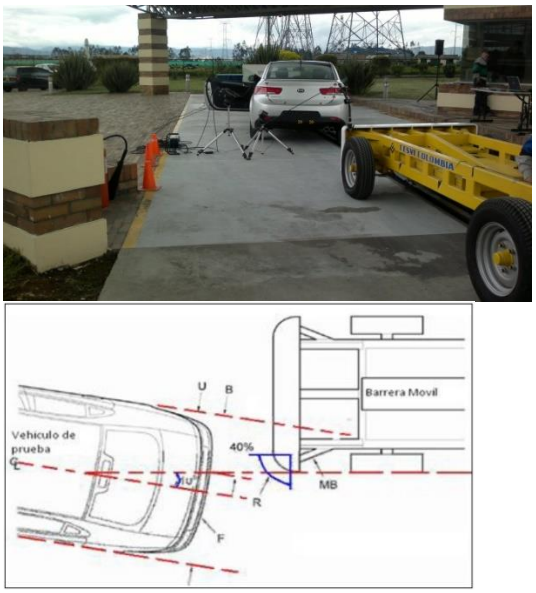

Figure 2. Left: scheme of rear impact; right: image of the rear impact test.

Where:
MB = moving barrier
H = height of barrier (700mm ±10mm)
h = height of barrier (200 mm ±10mm)
F = test vehicle
Radius R = Constant (150 mm)
Radius r = Constant (50 mm)
U = 40% compensation
B = total width of vehicle

2.3 Location of the mechanism

The mechanism must be placed inside the vehicle, aimed toward the brake pedal to be triggered; this condition proposes for the mechanism to be versatile, easily anchored, and for use in various types of vehicles that gather the conditions for the impact test study carried out by CESVI Colombia. To define the dimensions of the braking mechanism structure, it is necessary to study the dimensions of the floor of the vehicle in the front left part "driver's side", to dimension the braking mechanism structure (Table 1 and Figure 3).

Table 1. Nomenclature of dimensions on the passenger compartment floor

DIMENSION	DESCRIPTION
A	Height from the vehicle floor to the lower dashboard lining.
B	Length of vehicle floor from the seat attachment to the pedal controls.
C	Height from the floor to the highest part that driver's seat can be adjusted.
D	Height from the left side vehicle floor to the light lever housings.
E	Width of left side vehicle floor from the closure of rocker panel bracket (cierre del estribo) to the floor center console.

Left lateral image of the passenger compartment

Upper image of the left floor of the passenger compartment

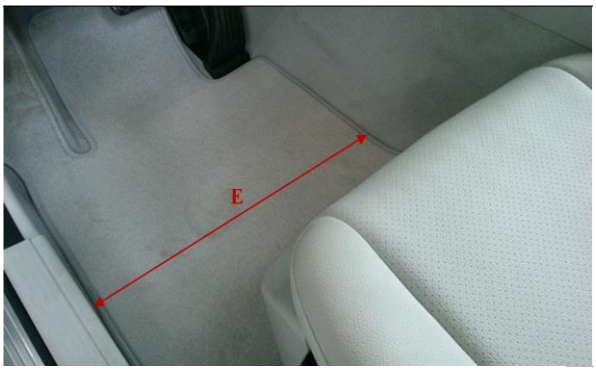

Figure 3.Schematic view of the dimensions indicated in Table 1..

3 Impact theory

Impact occurs when two bodies come into contact and collide together during a short period of time, producing strong impulsive forces among them.
Two types of impacts exist [4]; the first is the direct central impact that occurs in the direction of the motion toward the mass centers of the particles that collide.

The second type of impact considers the motion of one or both particles that form an angle with respect to the line of impact; this impact is known as oblique impact. The purpose of performing this analysis was to identify at what moment or distance the vehicle must stop without affecting the test protocol, not only guaranteeing that the vehicle stops, but that damages to the vehicles are not additional unforeseen matters in parts and labor.

3.1 Restitution Coefficient

The restitution coefficient is equal to the ratio between the relative speed of the separation of the mass centers just after the impact, $(\boldsymbol{V_B})_2$ - $(\boldsymbol{V_A})_2$, (Relative speed just after the impact) and the relative speed of the approach just before the impact $(\boldsymbol{V_A})_1$ - $(\boldsymbol{V_B})_1$ (Relative speed just before the impact). By experimentally measuring these speeds, it has been found that they vary appreciably from the impact speed, as well as in the size and shape of the bodies colliding [11]. Because of this, the restitution coefficient is reliable only when using data that closely approach existing conditions and when recording measurements. In general, a value is obtained of the restitution coefficient, with zero being a value where the two particles do not rebound (plastic) and one is the highest rebound value (elastic).

$$e = \frac{(V_{BM})_2 - (V_v)_2}{V_{v1} - V_{BM1}} \qquad (1)$$

e : restitution coefficient
V_{v1}: Initial speed of the test vehicle
V_{BM1}: Initial speed of the moving barrier
$(V_v)_2$: Final speed of the test vehicle
$(V_{BM})_2$: Final speed of the moving barrier

3.2 Impulse *and conservation of momentum*

Oblique central impacts occur when the trajectories of the bodies in contact are not perpendicular to the plane of impact. If the initial speeds are known of the moving barrier and the test vehicle, the equation would have two unknowns, $\boldsymbol{V_{v2}}$ and $\boldsymbol{V_{BM2}}$, that correspond to the final speeds just after the impact.

The value of $(V_{BM})_2$ was obtained with respect to the values measured with a laser speed sensor (CCLD, 3 – 20 mA MM-03) located between the test vehicle and the moving barrier; the purpose of this sensor is to measure the speed with which the moving barrier decelerates after impacting the test vehicle. The result of this measurement with respect to impacted vehicles yielded that the final speed of the moving barrier approximately through conservation of the linear momentum is $1{,}5\ m/s$ $(5{,}4\ Km/h)$.

Clearing of equation 2 yields the value of the final speed $(V_v)_2$ acquired by the vehicle after the trial; all this to replace the values in equation 1 and determine the restitution coefficient.

$$m_v\,(V_v)_1 + m_{BM}\,(V_{BM})_1 = m_v\,(V_v)_2 + m_{BM}\,(V_{BM})_2 \qquad (2)$$

Where:

m_v *= mass of the test vehicle*
V_{v1} *= initial speed of the test vehicle*
m_{BM} *= mass of moving barrier.*
V_{BM1} *= initial speed of the moving barrier:* $15\ km/h \pm 1\ km/h$.
$(V_v)_2$ *= final speed of the test vehicle*
$(V_{BM})_2$ *= final speed of the moving barrier*

Table 2 shows the value of the final speed of the test vehicle and the restitution coefficient with respect to the mass of the previously selected vehicles. Data are taken from prior tests conducted at CESVI Colombia.

By obtaining the restitution coefficient values, it is observed that decreased values exist when increasing vehicle mass, that is, the coefficient decreases for each of the vehicles from lower mass to greater mass. Instead, deceleration values diminish if the vehicle mass increases, as will be shown ahead.

4. Braking dynamics

The torque transmitted to the wheels generates a driving force (Fi), which transmitted to the vehicle mass provokes its final displacement.

The work developed in this displacement is equivalent to the vehicle's kinetic energy. Hence, the work will be equal to the force applied in the vehicle (Fi) during a distance travelled [3].

4.1 Stopping distance

The vehicle's stopping distance is the space a vehicle travels from the moment the braking system is activated until the vehicle comes to a complete stop. The distance the vehicle travels depends mainly on the following factors:

- Brake force (Ff)
- Friction coefficient (μ)
- Vehicle velocity (v)

To calculate the distance the vehicle travels until stopping, the following formula is used:

$$l = \frac{v^2}{E * 254} [meters] \quad (3)$$

Where:

l = *stopping distance [m]*
E = *l effectiveness of the brake system*
v = *velocity in [km/h]*

4.2. Vehicle deceleration

The deceleration produced during the braking process is calculated by applying formulas similar to those from the acceleration calculation, but anteceded by the minus symbol (–).

$$Desceleration, d = \frac{Deceleration}{Downtime} = -\frac{V\ initial - V\ final}{time} \quad (4)$$

Table 3 shows the results obtained from equations 3 and 4, which demonstrated the deceleration of the test vehicles with their stopping distances or calculated stop with respect to velocity and mass values for each vehicle.

Table 2. Results of the speed of test vehicles and restitution coefficients

Item	Make	Vehicle	Vehicle mass [Kg]	Final speed $(V_v)_2$ (m/s)	Restitution coefficient
1	Hyundai	i10	880	4.23	0.66
2	Renault	Duster 4x4	1359	2.48	0.39
3	Hyundai	i25 sedan	1560	2.16	0.34
4	BMW	5 Series Sedan	1685	2	0.31
5	Audi	A6 S6 4.0	1865	1.81	0.28
6	Dodge	Journey	1926	1.75	0.27
7	SsangYong	Actyon	1995	1.69	0.26
8	Chevrolet	Trailblazer A/T	2103	1.6	0.25
9	Jeep	Grand Cherokee	2335	1.44	0.22
10	Toyota	Land Cruiser Imperial	2630	1.28	0.2

Table 3. Deceleration results and calculated stopping distance

Item	Make	Vehicle	Vehicle mass [Kg]	Deceleration $[m/s^2]$	Distance [cm]
1	Hyundai	i10	880	-2.12	107.5
2	Renault	Duster 4x4	1359	-1.24	37
3	Hyundai	i25 sedan	1560	-1.08	28.08
4	BMW	5 Series Sedan	1685	-1.00	24.07
5	Audi	A6 S6 4.0	1865	-0.90	19.65
6	Dodge	Journey	1926	-0.88	18.42
7	SsangYong	Actyon	1995	-0.85	17.17
8	Chevrolet	Trailblazer A/T	2103	-0.80	15.45
9	Jeep	Grand Cherokee	2335	-0.72	12.53
10	Toyota	Land Cruiser Imperial	2630	-0.64	9.88

4.3. *Maximum brake force*

The maximum brake force (Ff_{max}) that must counteract against the driving force (Fi), depends on the weight of the vehicle (W) and on the adherence coefficient of the tires and the terrain (μ).

The brake force in each axle of the vehicle is proportional to the weight distribution on the axles.

$$Ff_{max} = W \cdot \mu \quad (5)$$

To calculate the maximum brake force, we begin by calculating the brake forces in each of the front and rear axles and, lastly, the total force to stop the vehicle, considering that the friction coefficient of the asphalt on the impact ramp is equivalent to that of new asphalt (0.85) [2]; this will be the condition to calculate the maximum brake force.

$$Ff_{max} = Ff_d + Ff_t \quad (6)$$

5 Pneumatic actuator

To select the pneumatic actuator, we must know the necessary force to activate the hydraulic brake system, bearing in mind that a person exerts a force of 100 N [3] with the right leg when stepping on the brake pedal; calculations are started to select the pneumatic actuator.

To determine the force and geometry of the piston of an actuator for forward and reverse gears, the following equations are used:

$$F_{advance} = P\left(\frac{\pi \cdot D_c^2}{4}\right) \quad (7)$$

$$F_{regression} = P\left(\frac{\pi \cdot D_c^2}{4} - \frac{\pi \cdot D_v^2}{4}\right) \quad (8)$$

Where:

D_c = *diameter of the cylinder*
D_v = *diameter of the stem*
P = *air pressure*

Bearing in mind after operating equations 7 and 8 with respect to the force required to trigger the brake pedal; the value of the diameter calculated for the cylinder was 24.46 mm, the pneumatic actuator is adjusted to 32 mm with respect to the Festo products normalized table [12].

5.1 *Electro-pneumatic design*

The following figure shows the electro-pneumatic assembly design that will trigger the mechanism's pneumatic actuator; to trigger the pneumatic actuator, a control element is used – which in this case is an electro-valve (5/2), which will be triggered by a module that emits an electric signal to the electric circuit and – in turn – the module will be commanded by a remote control that emits a radio frequency signal.

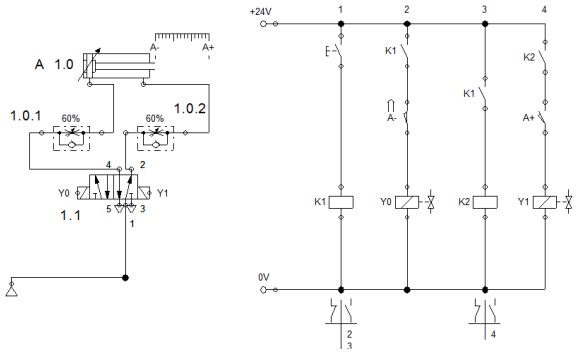

Figure 4. Electro-pneumatic design –FESTO Fluidism.

6. Design of the braking mechanism

Regarding the calculations carried out, we obtained a design base that finally resulted in the construction of the final device, but prior to this construction problems emerged pointing directly to the anchorage both inside the vehicle compartment and the fastening to the brake pedal, a system that would finally be used to stop the vehicle complying with the purpose of the test and adapting technologies in one mechanism to improve these types of crash-test trials.

6.1. Mechanism to fasten the mechanism

To anchor the braking mechanism to the vehicle for the purpose of restricting its movement, we used industrial grade fabric to cover the articulation and the form to adjust it to the brake pedal with two adjustable Velcro straps; this design permits does not depend on mechanisms that will try to adjust to different geometries of the brake pedals and will meet the objective of attaching the pneumatic actuator to the pedal. The following figure shows the model and its application to a brake pedal.

Figure 5. Left: rotating foot with cover; right: rotating foot attached to the brake pedal.

6.2. Electro-pneumatic braking mechanism

This section shows the mechanism in its final operating phase, designed solely to solve the need to stop test vehicles during impact tests carried out at CESVI Colombia. The following images show the virtual scheme for the assembly of the mechanism inside the compartment of a vehicle.

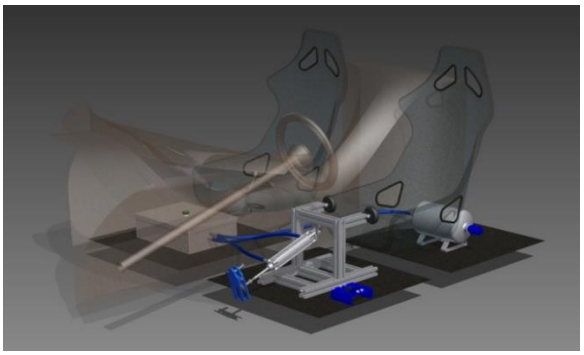

Figure 6. Virtual assembly of the braking mechanism - CESVI Colombia

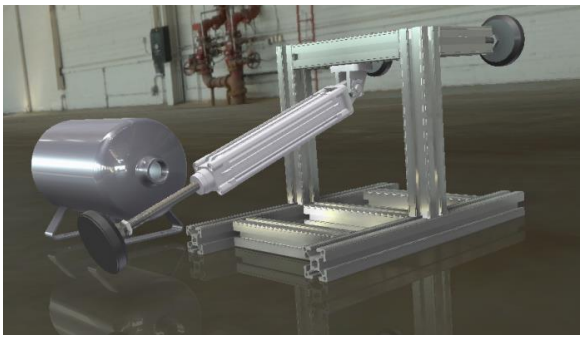

Figure 7. Braking mechanism - CESVI Colombia

The figures show the electro-pneumatic mechanism, which solves the need to stop test vehicles for impact tests at CESVI Colombia, besides being a safety mechanism for the tests performed there. The location or distribution of operation of the mechanism inside the vehicle compartment is described in the following manner.

- Structure with the actuator – Left frontal zone of the vehicle toward the brake pedal (floor).
- Compressed air tank – Left or right rear zone of the vehicle (floor).
- Electro-pneumatic control box – Right frontal zone of the vehicle (floor).

This type of device can be fitted to vehicles on the steering wheel on the right.

6.3. Performance of the mechanism during real tests

During the final phase of the mechanism's design and construction, it was necessary to run calibration and tuning tests for operation, that is, the assembly was installed on several vehicles to verify its functioning and versatility. To develop these tests, CESVI Colombia provided the physical and technical resources to validate the tests; the company loaned its test vehicles for the front and rear impact tests performed (Table 4).

Table 4. Assembly tests of the mechanism

Test vehicle	Date of trial	Does the mechanism fit?	Observations
Dodge Journey	09/11/2011	YES	Actuator position had to be changed
Chevrolet Cruze	10/11/2011	YES	N/A
Kia CERATO KOUP	22/06/2012	YES	N/A
Mazda 3 All New Sport	27/07/2012	YES	N/A
Kia Picanto ION	24/08/2012	YES	Actuator had to be calibrated
Kia Rio Spice	28/09/2012	YES	N/A.
Nissan March	16/11/2012	YES	Actuator had to be calibrated

The following test consists in the mechanism stopping the vehicle prior to it impacting the fixed barrier; for this test the final distance is revised until the vehicle comes to a complete stop. The data is compared with the calculated distance. Table 5 shows the difference of the calculated data vs. the distance measured.

The mechanism stopped the lighter vehicles at a greater distance, but due to the effect of the restitution coefficient they were travelling at higher speed; these small distances were not relevant, given that after being impacted in the rear the test vehicle never reached the impact barrier.

Table 5. Mechanism efficiency under real tests

Test vehicle	Weight of vehicle [kg]	Stopping distance during the trial [cm]	Theoretical stopping distance [cm]	Difference [cm]
Dodge Journey	1926	15	18.42	-3.42
Chevrolet Cruze	1461	28	32.01	-4.01
Kia CERATO KOUP	1560	25	28.08	-3.08
Mazda 3 Sport	1310	40	39.82	0.18
Kia Picanto ION	845	105	95.70	9.30
Kia Rio Spice	1041	70	63.06	6.94
Nissan March	960	76	74.15	1.85

Figure 8. Test vehicle rear impact (KIA Picanto ION); left: mechanism mounted in the test vehicle; right: impact test.

7. Conclusions

The electro-pneumatic mechanism was implemented, which will operate the braking systems on the test vehicles use don rear-impact tests carried out at CESVI Colombia S.A. After proposing preliminary designs to fasten the mechanism to the brake pedal, a design was implemented that permits perfectly fastening the pneumatic actuator to the brake pedal.

Through real trial son vehicles, the devise meets the operating expectations avoiding damage that would increase repair costs. The device implemented is characterized for its versatility, considering that it adapts to several vehicle models without incurring on configuration and assembly cost overrun.

Possible future research will be related to the simulation of collision events and conduct a validation with the data from reparability studies. The aforementioned would pose a new approach for reparability studies or an alternative method prior to the development of a crash test although at a high computational cost due to the system's dynamic complexity.

Acknowledgements

The authors wish to thank CESVI Colombia for all the logistics and financial support provided for the development of this project, besides trusting us with this work.

REFERENCES

[1] Research Council for Automobile Repairs, «RCAR Low-speed structural crash test,» July 2011. [En línea]. Available: http://www.rcar.org/Papers/Procedures/rcar_LowSpeedCrashTest2_2.pdf.

[2] V. A. Irureta, Accidentologia vial y pericia, Buenos Aires: La Rocca, 1999.

[3] CESVIMAP, «Manual de reconstrucción de accidentes de trafico,» 2006. [En línea]. Available: http://www.mapfre.es/wcesvimap/es/cinformativo/manual-de-reconstruccion-de-accidentes-de-trafico.shtml.

[4] R. C. Hibbeler, Mecánica vectorial para ingenieros, Dinámica, Mexico: Pearson Prentice Hall, 2004.

[5] F. Beer y J. Russell, Mecánica de materiales, Mexico: Mc Graw-Hill, 2006.

[6] R. Norton, Diseño de máquinas: segunda edición, Mexico: Pearson Prentice Hall, 1999.

[7] A. Guillén Salvador, Introducción a la neumática, Barcelona: Marcombo S.A., 1993.

[8] V. Kóczy, R. Annamária, A. Rövid y P. Várlaki, «Intelligent methods for car deformation modeling and crash speed estimation.,» de *The 1st Romanian-Hungarian Joint Symposium on Applied Computational Intelligence*, 2004.

[9] K. Fuerstenberg, P. Baraud, G. Caporaletti, S. Citelli, Z. Eltan , U. Lages y C. Lavergne, «Development of a Pre-Crash sensorial system –The CHAMELEON Project,» de *Proceedings of joint VDI/VW Congress: Vehicle 2nd Century of Automotive Technology*, Wolfsburg, 2001.

[10] A. Tejasagar, K. Srikanth y P. Veeraraju, «Simulation of vehicular frontal crash-test,» *International Journal of applied research in mechanical Engineering*, vol. 2, nº 1, 2012.

[11] R. Jazar, Vehicle Dynamics: Theory and Application, Springer, 2008.